Journal of Civil Engineering and Materials Application

Journal home page: http://jcema.com

Received: 03 April 2020 • Accepted: 26 July 2020

Research

doi: 10.22034/jcema.2020.241135.1033

Comfort Level Investigation of Chromite Composite Floor System under Human Walking Load

Farhad Abbas Gandomkar [*1] ,Mona Danesh [2]

[1] Department of Structure, Faculty of Civil Engineering, Jundi-Shapur University of Technology, Dezful, Iran.

[2] Department of Civil Engineering, Faculty of Engineering, ACECR Institute of Higher Education, Khuzestan, Iran.

*Correspondence should be addressed to Farhad Abbas Gandomkar, Department of Structure, Faculty of Civil Engineering, Jundi-Shapur University of Technology, Dezful, Iran.Tel: +986142428000; Fax: +986142428000; Email: farhad@jsu.ac.ir.

ABSTRACT

This paper's main objective is to determine the comfortableness of a composite structural floor system known as Chromite. For this purpose, twenty-eight Chromite panels were developed via the Finite Element Method (FEM) to find their Fundamental Natural Frequency (FNF). Then, the studied panels are categorized as Low-Frequency Floor (LFF) or High-Frequency Floor (HFF) regarding to their FNFs. Peak accelerations of low and high-frequency panels and also static stiffness of high-frequency panels were determined and compared with the limit value affirmed by the American Institute of Steel and Construction (AISC). Effects of various parameters were determined on changing FNF and also peak acceleration and static stiffness of the studied panels, depend to kind of panel as LFF or HFF. The results demonstrated that although some factors decreased and increased peak acceleration and static stiffness of the Chromite system, respectively, the panels could reach high vibration levels resulting in lack of comfortableness for users. In addition, the results show that the Chromite floor system needs to improve to be comfortable for users.

Keywords: Chromite floor system, comfortableness, human walking load, static and dynamic response, low and high frequency floor.

1. INTRODUCTION

Human comfort is an important aspect that needs to be considered in the design of structural floor systems. Any local minor damages, weakness of structural or nonstructural components, or extreme movements of structures affect the human comfort level [1-2]. Floors of buildings will not be suitable for human occupancy since users feel uncomfortable. Therefore, the aspect of human comfort must be carefully addressed in the design of floor buildings. The vibration of structural flooring systems can be a critical criterion affecting human comfort, and this is normally generated by human activities (in residential buildings, offices, hotels, and so on) and also by machineries (in industrial buildings) placed on the floor. Alvis in 2001 [3] stated that Treadgold was the first person to study the vibration of floors under the human walking load in 1828. Also, Postlethwaite in 1944 determined the vibration perception threshold as 'feel'-'no feel' by only 0.03% of g for the floor with the FNF lower than 10 Hz, which is much lower than the

idea of Mallock at the beginning of the nineteenth century. Mallock presented this threshold by word of 'noticeable' with 1% of g. However, the exact meaning of noticeable was not explained. In addition, Dieckmann (1958) experimentally determined the vibration perception threshold as 0.4% of g. Furthermore, Pretlove (1991) and Rainer (1995) respectively compiled data from different sources and proposed a vibration perception threshold for peak acceleration as 0.34% g, and they referred to it as "just perceptible". Eriksson (1994) carried out a similar exercise by compiling all available data based on RMS accelerations for offices and deduced that acceptable RMS acceleration levels are 0.02-0.06 m/s2 (0.2-0.6% g), depending on the type of offices labeled as "special", "general" or "busy" [4]. In addition, according to Gandomkar in 2012 [5], various codes presented criterion to define comfortableness of floors for various applications such as schools, residential houses, and offices when the human walking load applied to them. The mentioned codes are such as Appendix G of the Canadian Standards Association Standard CSAS16.1 (CSA), Steel Construction Institute (SCI-P354), NRCC 28482, BS 6472, American Society of Civil Engineers (ASCE 7-05) in its Appendix C, the National Research Council Canada 32349 (NRCC) (Allen and Rainer 1976, Allen et al. 1987, The Steel Construction Institute 2007, BS 6472. 1992, ASCE/SEI 7-05. 2006). Furthermore, the International Standards Organization (ISO 2631-2) [6] recommended limits as a baseline in terms of RMS acceleration and multiples of baseline curve in terms of peak acceleration to make floors comfortable under human activities, as illustrated in Figure 1 [6]. As it is shown in Figure 1, the peak acceleration limits are obtained by multiplying the baseline with 10 for offices and residences, 30 for indoor footbridges, shopping malls, as well as floors used in dining and dancing, and 100 for outdoor footbridges and floors used in rhythmic activities. American Institute of Steel Construction (AISC) in 11th Steel Design Guide Series, proposed the recommendation of ISO 2631-2 for floors and stated that the reaction of people who feel vibration depends on their activities [7]. People in offices or residences, and those who take part can respectively accept peak accelerations of about 0.5 and 5 percent of the acceleration of gravity (g). Moreover, people dining beside a dance floor, lifting weight beside an aerobics gym, or standing in a shopping mall may accept peak acceleration equal to 1.5 percent of g. Allen and Murray (1993) presented the same suggestion likeness the AISC, a limit state of ISO 2631-2 for offices and commercial buildings when user walk across the floor [6].

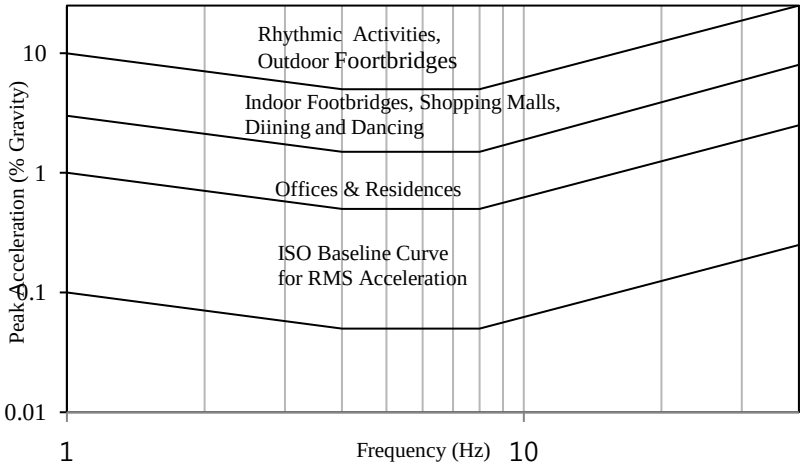

Figure 1. Recommended peak acceleration for human comfort for vibrations due to human activities [6]

Several studies have been carried out on the dynamic performance and behavior of various structural floor systems under human activities. An et al. in 2016 presented dynamic performance characteristics of an innovative composite floor system known as CSBS-CSCFS, under human-induced load. They found experimentally that vibration of the mentioned floor was affected by some parameters such as dynamic characteristics of the floor, type of human-induced load, stationary people occupying the floor, synchronism of activities, crowd size, and load frequency. They compared the results of dynamic responses of the studied floor with ISO and AISC criteria to present the comfortableness of the studied floor system [8]. Gaspar et al. in 2016, investigated the dynamic behavior of building a steel-concrete composite floor system when human rhythmic activities were applied on the floor. They found the studied floor system can reach high vibration levels that can compromise the user's comfort. They also installed and simulated a multiple tuned mass damper to provide human comfort [9]. Weckendorf et al. in 2016 uncovered vibration serviceability performance of timber floor system. They stated that control of acceptable floor vibrations is a part of some current timber design standards, however, a universal agreement on acceptance levels and design procedures have not been achieved yet. Therefore, the authors presented an overview of traditional and recent design approaches for timber floor vibrations to allow engineers to check the design strategies of floor production [10]. Zhou et al. in 2016 studied on vibration serviceability of the pre-stressed cable RC truss floor system. They found that the studied system was in the category of LFF with a low damping ratio (damping ratio of less than 2 percent). By comparing the experimental results with the AISC limits, it was shown that the system was exhibited satisfactory vibration perceptibility [11]. Carmona et al. in 2017, used a tuned mass damper with friction damping to control excessive floor vibrations. They performed experimental tests by doing rhythmic activities of

continuous jumping, walking randomly, and synchronized movements with semi bended knees. The results affirmed that the tuned mass damper could reduce the response acceleration of the studied floor system [12]. Friehe et al. in 2017, presented an assessment method to design floors with highly vibration-sensitive equipment. To achieve their aim, they considered different walking loads. The results visualized graphically to predict the floor vibration due to human load [13]. Shahabpoor et al. in 2017 presented a new design framework to evaluate human-structure interaction. They proposed a more reliable method for serviceability assessment of the vertical vibrations induced by multi-pedestrian walking traffic. Also, they studied on the modeling of natural variability of the walking forces and human bodies. In addition, they proposed a novel approach to evaluate vibration serviceability assessment based on the actual level of vibration experienced by each pedestrian [14]. Andrade et al. In. 2017, studied the vibrations of a staircase of a building under human activities. They measured the dynamic response of the staircase, experimentally. Then, they reinforced the staircase to decrease its vibrations [15]. Zhang in 2017 in his Ph.D. thesis, worked on vibration serviceability of cold-formed steel floor system. He stated that four important aspects have an effect on studied floor vibration performance: rotationally restrained floor joist ends, structural properties of the floor system, human-structure interactions, and the applicable design guidelines. He also developed design guidelines for the lightweight steel floor system in residential constructions [16]. Zhang et al. in 2017, studied modeling, formulation, and dynamic properties of lightweight steel floor systems with human occupants. They proposed a damped plate-oscillator model to achieve dynamic properties of the coupled floor-occupant system. They investigated the influence of human occupants on the dynamic properties of lightweight steel floors in three scenarios: an unoccupied floor, a floor with one standing occupant, and a floor with two standing occupants [17]. Mohammed et al. in 2018, developed an improved model to uncover human-induced vibrations of high-frequency floors. They found that the improved model shifted the suggested cut-off frequency between low and high-frequency floors from 10 Hz to 14 Hz. In addition, their results showed that while the existing model presented overestimate or underestimate vibration levels depending on the pacing rate, the new model offered statistically reliable estimations of the vibration responses [18]. Casagrande et al. in 2018 worked on the analytical, numerical, and experimental assessment of vibration performance in the timber floor system. They presented the assessment of dynamic properties and vibration performance of two full-scale timber floor specimens: Timber-Concrete Composite floor and Cross Laminated Timber floor [19]. Do et al. in 2018, presented a novel framework for vibration serviceability assessment of stadium grandstands, considering durations of vibrations. They stated the currently available approaches using raw acceleration, weighted RMS acceleration, vibration dose values, and so on may not always be sufficient for serviceability assessment due to the lack of guided procedure for calculating the integration time and implementing the duration of vibration into the process. Therefore, they proposed a new parameter and framework for assessing human comfort, which incorporated the duration of vibration with conventional data processing. This parameter was the area of RMS [20]. Campista and da Silva in 2018 studied the vibration behavior of the steel–concrete composite floor system when the floor was subjected to rhythmic human activities. They performed the experimental test and numerical analysis to evaluate the dynamic response of the floor system. Based on the current human comfort criteria, they measured the peak accelerations, RMS, and vibration dose values to evaluate the human comfort level of the studied system [21]. Cao et al. in 2018 presented a review of research on human-induced vibration serviceability and dynamic properties of long-span floor systems [22]. Zhou et al. in 2018, studied the human-induced vibration serviceability of the arch pre-stressed concrete truss system. They stated that experimental results showed the system was in the category of HFF with a low damping ratio [23]. Chen et al. in 2018, studied the human-induced vibration of the steel–concrete composite floor system. For this purpose, a finite element study was conducted to evaluate the dynamic response of the system under human walking and rhythmic activities. The results indicated that human-induced vibration of the system was influenced by several factors, namely the load model, the floor's natural frequency, effective weight, and damping ratio [24]. Wang in 2018, in his Ph.D. thesis, studied on a vibration control strategy, to abolish floor vibration by the internal mass damper. For this aim, he built an in-service dining hall floor and a full-scale laboratory floor structure, during his thesis. He used a finite element and experimental method to achieve the results [25]. Hassanieh et al. in 2019, studied the vibration behavior of the steel-timber composite floor system. They performed a dynamic analysis of the studied system under human activities to predict the vibration behavior of the mentioned floor system. They also presented some floor design recommendations to ensure the satisfactory performance of the studied floor system according to existing building codes [26]. Chiniforush et al. in 2019, presented experimental and numerical investigation on the vibration behavior of the steel-timber composite floor system. Modal testing and numerical analysis were carried out on six models of the studied floor system, and then the acceleration response, natural frequencies, damping ratios and mode shapes were measured [27]. Ebadi et al. in 2019, studied the evaluation of floor vibration caused by human walking in a large glued-laminated-timber (glulam) beam and office floor. Their results uncovered that topping layers, presence of office workers, and furniture strongly influenced on FNF and damping of the system [28]. Abdeljaber et al. in 2019, worked on a novel video-vibration monitoring system for walking pattern identification on floors. The system was capable of capturing occupant movements on the floor with cameras, and extracting walking trajectories using image processing techniques. To determine its capabilities, the system was installed on a real office floor, and resulting trajectories were statistically analyzed to identify the actual walking patterns, paths, pacing rates, and busyness of the floor with respect to time [29]. Goncalvez et al. in 2019, presented a literature review on vibration serviceability assessment of office floors for realistic walking and floor layout scenarios [30]. Royvaran et al. in 2020, investigated the accuracy of four simplified methods by comparing predicted and observed acceptability

of 50 framed floor with W-shaped members subjected to walking excitations [31]. Huang et al. in 2020 studied on the vibration of a cross-laminated timber floor system under different boundary conditions. They investigated the dynamic response of the mentioned floor system by considering the effect of beam spacing, beam size, and supporting conditions on the behavior of the floor system. They established an analytical model to enable engineers to quickly estimate the relevant dynamic properties of the studied floor system with different boundary conditions [32]. Li et al. in 2020, presented a method for calculating uncomfortable rates of people subject to vertical floor vibrations based on fuzzy reliability theory. They obtained uncomfortable rates corresponding to different acceleration limits and functions for the design factor method of buildings [33]. Zhang et al. in 2020 studied the vibration performance of U-shaped steel-concrete composite hollow waffle slab by two experimental and analytical methods. They stated modal properties of the system showed the system was in the category of LFF with a low damping ratio [34].

In accordance with Middleton and Brownjohn [35], there is little energy in the higher harmonics after four harmonics of a walking force (approximately 10 Hz). A floor is HFF, if it has a FNF above 10 Hz. But, it is known as a LFF if it is dominated by resonance from the first four harmonics of a walking force. Ljunggren et al. [36] stated that some researchers suggested two different design criteria for the floor; deflection criteria for HFF and an acceleration limit for LFF. However, the AISC [7] recommended an acceleration limit for LFF and HFF and a minimum static stiffness of 1 kN/mm under concentrated load as an additional check for HFF.

This paper deals with the response of low and high-frequency Chromite floor system (Figure 2), used as offices and residences, under human walking load to determine its comfortableness. Twenty-eight Chromite panels were studied to reveal the effect of various parameters such as dimension of the panel, boundary conditions, the rigidity of main and secondary beam, adding tie beam, the thickness of the concrete slab, the height of composite joist, space between the joists, grade of concrete, damping of the floor panel, and type of path, on changing FNF and also static and dynamic response of low and high-frequency Chromite floor system. To achieve the main objective of this study, firstly, natural frequencies and vibration modes of all studied panels were obtained. Secondly, regarding suggestion of the AISC, peak acceleration of studied LFFs and also static stiffness and peak acceleration of studied HFFs were determined and compared with limiting values, affirmed by the AISC [7].

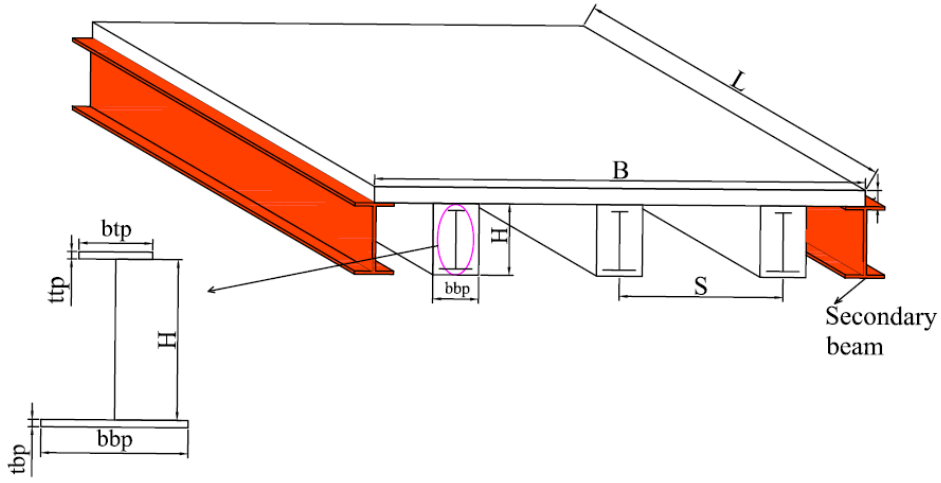

Figure 2. Chromite floor system

2. MATERIALS AND METHODS

In this section, first, structural models consisting of characteristics of panels and their material properties and also human-induced dynamic loads are presented. Second, methods of analysis and checking of comfortableness of models are stated. Third, a verification study is presented.

2.1. STRUCTURAL MODELS

2.1.1. Characteristics of Chromite Panels

The structural model of the system is shown in Figure 2. The characteristics of the studied panels are presented in Table 1. Boundary conditions (B.Cs) of the studied panels, shown in the last column of Table 1, are illustrated in Figure 3. The grade of concrete is 30 (C30) in the PN1 till PN27, but this grade is C35 in the PN28.

Table 1: Characteristics of Chromite panels

Panel Name	L (mm)	B (mm)	H (mm)	t_{bp}, t_{tp} (mm)	t (mm)	S (mm)	Number of tie beam	Main Beam	Secondary Beam	Number of Secondary Beam	B.Cs
PN1	4000	6000	220	5	50	500	-	240	240	2	B.C.1
PN2	4000	6000	220	5	50	500	-	180	180	2	B.C.1
PN3	4000	6000	220	7	50	500	-	240	240	2	B.C.1
PN4	4000	6000	220	5	100	500	-	240	240	2	B.C.1
PN5	4000	6000	220	5	50	500	-	240	240	2	B.C.2
PN6	4000	6000	220	5	50	500	-	240	240	2	B.C.3
PN7	4000	6000	220	5	50	500	-	240	240	2	B.C.4
PN8	4000	6000	220	5	50	500	-	240	240	2	B.C.5
PN9	4000	6000	220	5	50	500	-	240	240	2	B.C.6
PN10	4000	6000	220	5	50	600	-	240	240	2	B.C.1
PN11	4000	6000	220	5	50	500	-	240	240	5	B.C.1
PN12	4000	6000	220	5	50	500	-	270	270	5	B.C.1
PN13	6000	6000	220	5	50	500	-	240	240	2	B.C.1
PN14	6000	4000	220	5	50	500	-	240	240	3	B.C.1
PN15	6000	4000	220	5	50	500	-	240	240	7	B.C.1
PN16	6000	4000	220	5	50	500	-	240	240	13	B.C.1
PN17	4000	6000	200	5	50	500	-	240	240	2	B.C.1
PN18	8000	6000	220	5	50	500	-	240	240	2	B.C.1
PN19	2000	6000	220	5	50	500	-	240	240	2	B.C.1
PN20	6000	3000	220	5	50	500	-	240	240	2	B.C.1
PN21	6000	7000	220	5	50	500	-	240	240	2	B.C.1
PN22	4000	6000	220	5	50	500	-	140	240	2	B.C.1
PN23	4000	6000	220	5	50	500	1	240	240	2	B.C.1
PN24	4000	6000	220	5	50	500	3	240	240	2	B.C.1
PN25	4000	6000	220	5	50	500	-	240	240	3	B.C.1
PN26	4000	6000	220	5	50	500	-	240	180	2	B.C.1
PN27	4000	6000	220	5	50	500	-	240	140	2	B.C.1
PN28*	4000	6000	220	5	50	500	-	240	240	2	B.C.1

*PN28: All characteristics are same as PN1 but the grade of concrete is C35.

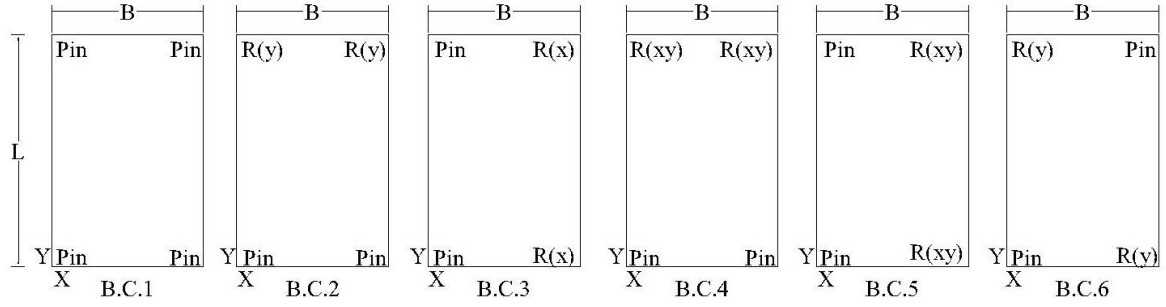

Figure 3. Boundary conditions of the studied panels

2.1.2. Properties of Materials

In this study, dynamic Young's modulus of materials was used as an input of finite element models. According to AISC, the dynamic Young's modulus for steel can be chosen similar to its static value, i.e. 2.10×105MPa [7]. Also, in accordance with BS 8110, the static Young's modulus of concrete was determined as 24597 MPa for grade 30 concrete [37]. Da Silva et al. discussed that according to the AISC, in situations where the composite slab is subjected to dynamic excitations, concrete becomes stiffer than the case when it is subjected to pure static loads [7,38]. This issue suggests a 35% increase in Young's modulus of conventional concrete [38]. Therefore, in this study, a 33206 MPa dynamic modulus of elasticity was adopted for grade 30 concrete. The Poisson's ratios were adopted as 0.3 for steel and 0.2 for concrete. Also, the density of steel and concrete was chosen 7850 kg/m3 and 2273 kg/m3, respectively [39-40].

2.1.3. Human-Induced Dynamic Loads

The vibration of floors under human rhythmic activities is a very complex problem with respect to mathematical or physical characterization of this phenomenon because the properties of dynamic vibration of these activities are interconnected to the individual body adversities and the ways which human performs a certain rhythmic activity [41]. A number of studies tried to introduce dynamic loads representing human activities. These studies are summarized in the study of Gandomkar in 2012 [5] and Gandomkar et al. in 2011 and 2012 [39-40]. In the current study, dynamic responses of the studied panels were determined under the following four dynamic human walking loads to evaluate their vibration acceptability [39-40].

2.1.3.1. First Load Mode

First load model which represents people walking is shown by Gandomkar et al. in 2011 and 2012 [39-40].

$$F(t) = P\alpha_i \cos(2\pi i f_s) \qquad (1)$$

Where:

P: Individual's weight, taken as 700-800 N;

α_i: Dynamic coefficient for the ith harmonic force component;

i: Harmonic multiple of the step frequency;

f_s: Step frequency;

t: Time in seconds.

In the first load model, only one resonant harmonic of the load was considered. The harmonic multiple of the step frequency was adopted from Table 2, which depends on the FNF of the panel. For example, if calculated FNF of a panel is equal to 5.2271 Hz (Panel Number (PN) of 1 = PN1), according to Table 2, the only third harmonic of the walking loads with step frequency of f_s =1.74 Hz (3 × 1.74 Hz = 5.2271 Hz) should be used in Eq. (1) to determine the first applied load on the panel. Figure 4 illustrates the first dynamic load model for the panel with FNF of equal to 5.2271 Hz.

Table 2. Loading frequencies, dynamic coefficients, and harmonic phase angles [41]

Harmonic i	Person walking			
	if_s (Hz)	α_i	Φ	
			Second and third load model	Fourth load model
1	1.6-2.2	0.5	0	0
2	3.2-4.4	0.2	$\pi/2$	$\pi/2$
3	4.8-6.6	0.1	$\pi/2$	π
4	6.4-8.8	0.05	$\pi/2$	$3\pi/2$

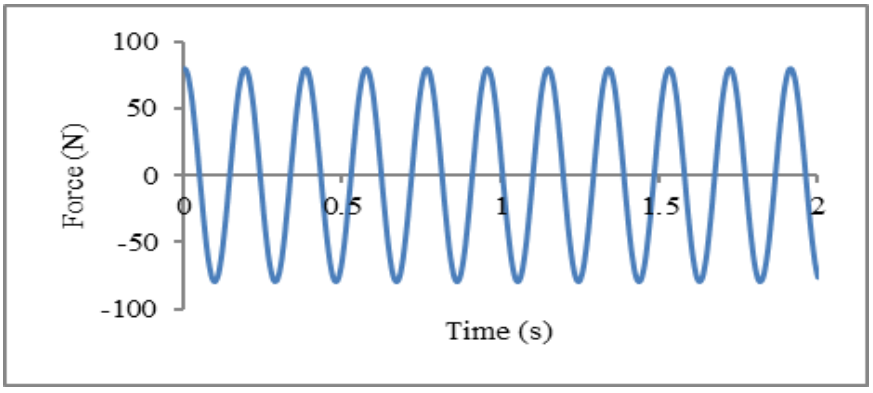

Figure 4. First load model for PN1

2.1.3.2. Second Load Model

The second load model that represents human walking load is presented as below [39-40].

$$F(t) = P[1 + \sum \alpha_i \cos(2\pi i f_s t + \Phi_i)] \quad (2)$$

Where:

P: person' weight;

α_i: Dynamic coefficient for the harmonic force;

i: Harmonic multiple ($i = 1, 2, 3, \dots, n$);

f_s: Activity step frequency (dancing, jumping, aerobics or walking);

t: Time;

Φ_i: Activity step frequency (dancing, jumping, aerobics or walking);

Unlike the previous load model, this load was composed of a static parcel and a combination of four time-dependent repeated loads presented by the Fourier series. Four harmonics (see Table 2) were adopted to produce the dynamic second load model. Considering a panel same as the discussed panel in the previous load model with the FNF equal to 5.2271 Hz, the third harmonic with a step frequency of 1.74 Hz (3 × 1.74 Hz = 5.2271 Hz) was the walking load resonant harmonic. Table 2 shows the dynamic coefficients and phase angles for each harmonic, which were used to produce the second dynamic load model, as depicted in Figure 5.

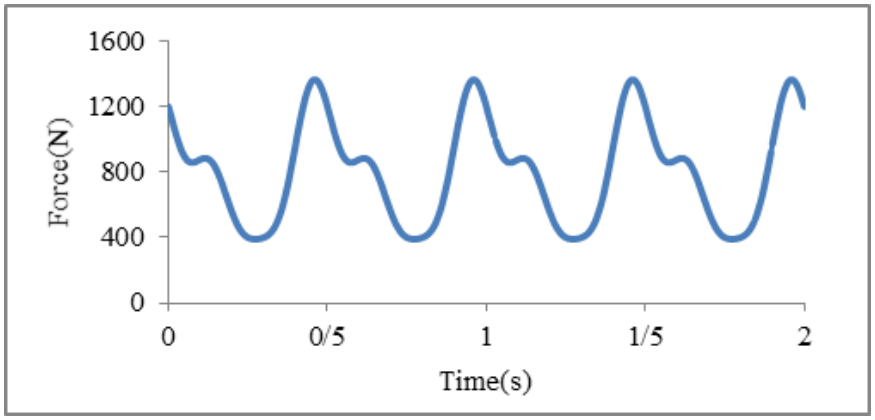

Figure 5. Second and third load models for PN1

2.1.3.3. Third Load Model

The mathematical function of the third load model, which represents the human walking load is similar to the second one, presented in Eq. (2). Similar to the previous load model, the third harmonic with a step frequency of 1.74 Hz was is the resonant harmonic of human walking load (see Table 2). The third load model is more pragmatic than the last two kinds of load models, as the position of this load changes across the singular location of the floor system (see Figure 6).

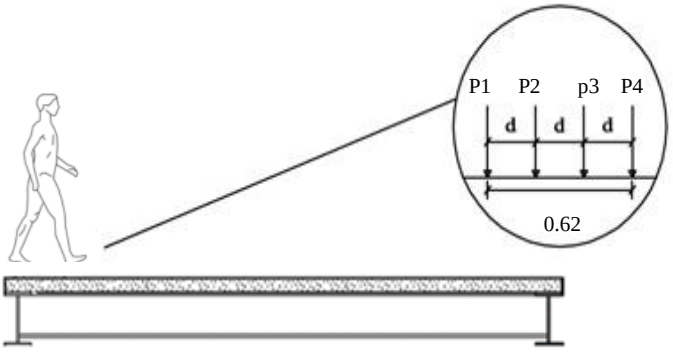

Figure 6. Person walking on the Chromite floor panel

In this kind of load, the study of some other parameters related to the step frequency such as step distance and speed of walking, presented in Table 3, is necessary. Also, the finite element mesh should be very fine in the third dynamic load model. The contact time of application of the dynamic load with the floor was calculated from the step distance and step frequency (see Table 3). In this load model, the subsequent scheme was followed: In a panel identical to the panel in the

previous load models, and according to Table 3, the step frequency was equal to 1.74 Hz when the third harmonic was as the resonant harmonic. Therefore, according to Table 3, the step distance was equal to 0.62 m (see Figure 6).

Table 3. Person walking characteristics [41]

Activity	Velocity (m/s)	Step distance (m)	Step frequency (Hz)
Slow walking	1.1	0.6	1.7
Normal walking	1.5	0.75	2.0
Fast walking	2.2	1.0	2.3

The step period which corresponds with the step distance of 0.62 m is equal to 1/f = 1/1.74 = 0.57 s (see Table 3). As shown in Figure 6, four forces were considered representing one human step, which each of the forces as P1, P2, P3, and P4 was applied on the floor during 0.57(contact time)/3 = 0.19 s. The dynamic forces of P1, P2, P3, and P4 were not applied together at the same time. First, the load of P1 was applied to the floor, according to Eq. (2) for 0.19s. At the end of this time period, the load of P1 became zero, and the load of P2 was applied for 0.19 s. The other loads of the first person step, P3 and P4, were applied in the same procedure described previously. After 0.57 s, the first person step finished, and the second person step started, and a load of P1 of the second step was equal to the load of P4 in the first step. According to the mentioned method, the process continued repeatedly untill all dynamic forces applied along the considered path (see Figure 11) of the floor.

2.1.3.4. Fourth Load Model

The fourth dynamic load model representing the human walking load is investigated with the same procedure considered in the third one. The principal difference between the third and fourth loads was the consideration of the human heel effect in the fourth load, which was ignored in the third load model. The human heel effect was uncovered to be an effective parameter on the increase of the load by comparison of the third and fourth load models. According to Mello et al. and Gandomkar et al., Varelo (2004) proposed the mathematical functions of the fourth load model as Eqs. (3-6) [39-41].

$$f(t) \qquad (3)$$

$$\begin{cases} \left(\frac{f_{mi}\,F_m - P}{0.04T_p}\right) t + P & \text{if } 0 \le t < 0.04T_p \\ f_{mi}\,F_m\left[\frac{C_1\left(t - 0.04T_p\right)}{0.02T_p} + 1\right] & \text{if } 0.04T_p \le t < 0.06T_p \\ F_m & \text{if } 0.06T_p \le t < 0.15 \\ P\left[1 + \sum_{i=1}^{nh} \alpha_i \sin(2\pi i f_s\,(t + 0.1T_p) + \Phi_i)\right] & \text{if } 0.15T_p \le t < 0.90T_p \\ 10(P - C_2).\left(\frac{t}{T_P} - 1\right) + P & \text{if } 0.90T_p \le t < T_p \end{cases}$$

F_m: Maximum Fourier series value, given by Eq. (4);

f_{mi} : Heel-impact factor;

T_p: Step period;

C_1: Coefficients given by Eq. (5);

C_2: Coefficients given by Eq. (6).

$$F_m = P\left(1 + \sum_{i=1}^{nh} \alpha_i\right) \quad (4)$$

$$C_1 = \left(\frac{1}{f_{mi}} - 1\right) \quad (5)$$

$$C_2 = \begin{cases} P(1 - \alpha_2), & \text{se } nh = 3 \\ P(1 - \alpha_2 + \alpha_4), & \text{se } nh = 4 \end{cases} \quad (6)$$

Mello et al. and Gandomkar et al. reported that Varela (2004) and Ohlsson (1982) declared the impact factor varies person-to-person. In this study, the heel-impact factor was adopted equal to 1.12 [39-41]. Figure 7 shows the dynamic load model of a panel which presented in the previous load models with the FNF of 5.2271 Hz, based on Eqs. (3)-(6).

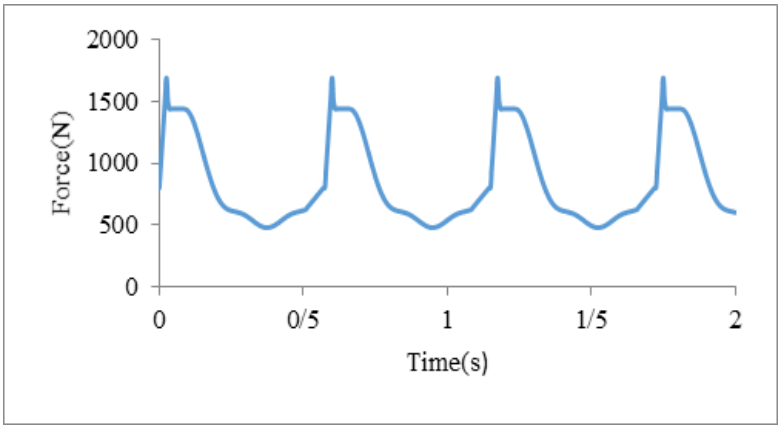

Figure 7. Fourth load model for PN1

2.2. METHODS OF ANALYSIS AND CHECKING OF COMFORTABLENESS

The FEM presents a more accurate dynamic response, especially for structures with involved geometry. Using this method is increased because it can reduce the cost of computing functions [42]. Therefore, in this study, the FEM was used to achieve the aims of the study. Developed finite element models were simulated by the use of fine mesh in the ABAQUS program [42]. To achieve the main aim of the paper, firstly, natural frequencies of the Chromite panels were determined through the development of a finite element model by the implementation of the ABAQUS program [42]. The developed finite element model was analyzed by "Modal analysis". The "Block Lanczos" method was used to obtain undamped natural frequencies of the studied system. Secondly, regarding the affirmation of the AISC, dynamic analysis was performed on the LFF panels and also dynamic and static analysis were performed on the HFF panels. The results of the analysis were peak accelerations for the LFF panels, and also peak accelerations and static stiffness for the HFF panels. Determined peak accelerations of the LFF and HFF panels were compared with the affirmation of the AISC (Figure 1). Also, the AISC, introduced a minimum static stiffness of 1kN/mm under concentrated load as an additional check of the HFF panels. Therefore, static stiffness of the HFF panels were estimated by finite element models and compared with the mentioned criterion of the AISC [7].

2.3. VERIFICATION STUDY

As stated, two various analyses were performed to achieve the main objective of this paper; static and dynamic. Therefore, in the case of verification study, first, static and dynamic computational models are prepared. Then, the results of them compared with the results of the affirmation of the AISC [7]. For this purpose, the PN1 has been selected to define the accuracy of the results of finite element models. The finite element models of the panels were prepared based on their material properties mentioned before and the type of elements. In the studied system, the concrete slab and also top and bottom plate of open web steel joists were assigned by the S4R shell element. In addition, concrete between composite joists and also tie beams were represented by the C3D8R solid element. In the end, the main and secondary beam were modeled by the B31 beam element.

2.3.1. Static Verification Study

The boundary conditions and finite element model of the PN1 is illustrated in Figure 8 and Figure 9.

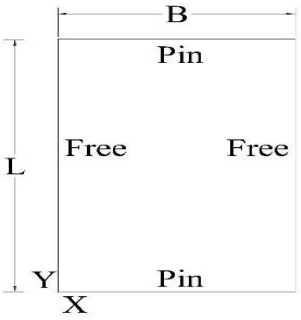

Figure 8. Boundary condition of verified panel

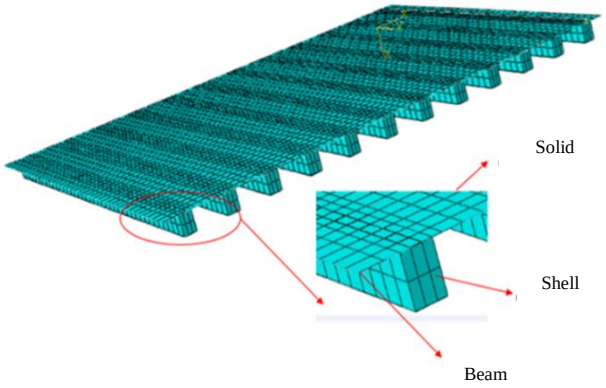

Figure 9. Finite element mesh of PN1

According to the AISC, a 1 kN concentrated load was applied to the center of the panel [7]. Static analysis was performed on the simulation, and the deflection of the center was determined by 0.03736 mm. According to the AISC, a floor with the boundary conditions at the two ends of the floor (same as shown in Figure 8) can be represented by a beam. The AISC proclaims a formula to calculate the deflection of mid-span of a beam as Eq. (7).

$$\Delta = \Delta_j + \Delta_g = \frac{PL_j^3}{48EI_j} + \frac{PL_g^3}{48EI_g} \quad (7)$$

Where:

Δ_j and Δ_g: Maximum deflection of the beam or joist and girder, respectivaly

P: Constant force equal to 1 kN

L_j: the length of floor

L_j: the width of floor

I_j: Moment of inertia along the length

L_j: Moment of inertia along the width

E: module of elasticity

The Eq. (7) has been used to calculate the deflection of the center of PN1, which is determined by 0.03600 mm. Comparing the results of FEM and the mathematic formula is shown a difference by 3.5%. Therefore, the error of the finite element model is acceptable, and so the model can present static results with good accuracy.

2.3.2. Dynamic Verification Study

In the case of verification study for the dynamic analysis of the studied system, FNF of the PN1 which determined by FEM was compared with FNF of the mentioned panel which calculated by fundamental mathematicformula, presented by the AISC This formula (Eq. (8)) is used to calculate FNF of a simply supported steel framed floor system [7].

$$f = \frac{\pi}{2}\sqrt{\frac{gEI}{WL^4}} \qquad (8)$$

Where

f: FNF (Hz)

g: Acceleration of gravity (9.806 $^{m}/_{s^2}$)

E: Modulus of elasticity of steel

I: transformed moment of inertia

W: Uniformly distributed weight per unit length (actual, not design, live and dead loads) supported by the member

L: Member span

As a result, FNF of the PN1 was determined by 36.384 Hz and 36.44 Hz from the finite element model and Eq. (8) respectively. Therefore, the error of the FEM was calculated by 0.15%. The mentioned error shows that the developed finite element model can predict the FNF of the system with high accuracy. On the other hand, the first four vibration modes of the PN1 are shown in Figure 10. The first mode of vibration is the bending mode, which shows the correct behavior of the studied panel.

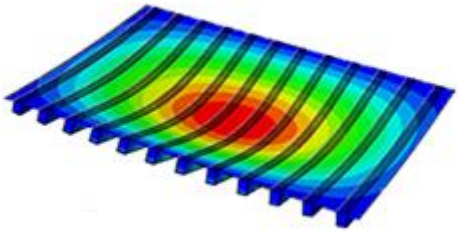

(a) Mode shape associated to the first Natural frequency. f_{01}=36.384 Hz

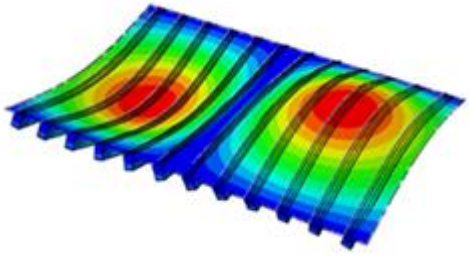

(b) Mode shape associated to the second Natural frequency. f_{02}=37.318 Hz

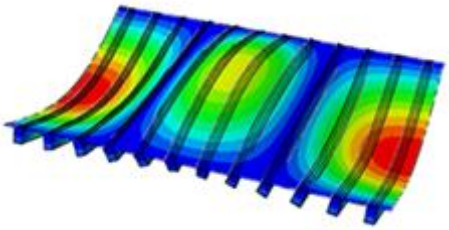

(c) Mode shape associated to the third Natural frequency. f_{03}=38.810 Hz

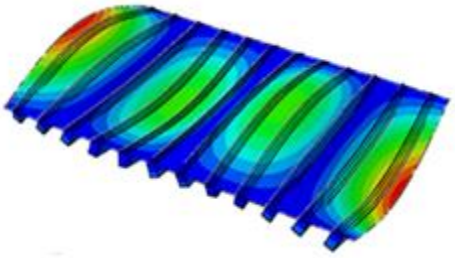

(d) Mode shape associated to the fourth Natural frequency. f_{04}=41.037 Hz

Figure 10. Floor vibration modes of PN1

3. RESULTS AND DISCUSSION

3.1. FNFS OF THE STUDIED PANELS

The studied panels should be categorized as LFF or HFF based on their FNFs to determine the type of their analysis. In addition, the FNFs of the panels are used for their dynamic analysis. The FNFs of the studied panels and their categorization is presented in Table 4. In this Table, the PN1 is considered as the base panel, which the FNFs of other panels are compared with its FNF.

Table 4. FNF and categorization of studied panels

Panel Number	FNF (Hz)	Category	PD (%)	Panel Number	FNF (Hz)	Category	PD (%)
PN1	5.2271	LFF	0	PN15	10.255	HFF	96.2
PN2	3.3802	LFF	-35.3	PN16	11.146	HFF	113.2
PN3	5.1772	LFF	-0.95	PN17	5.3367	LFF	2.1
PN4	5.5882	LFF	6.9	PN18	3.6673	LFF	-29.8
PN5	6.4604	LFF	23.6	PN19	7.1159	LFF	36.1
PN6	5.2278	LFF	0.01	PN20	12.191	HFF	133.2
PN7	6.4606	LFF	23.6	PN21	6.4706	LFF	23.8
PN8	7.8817	LFF	50.9	PN22	2.4961	LFF	-52.2
PN9	7.9935	LFF	52.9	PN23	6.5285	LFF	24.9
PN10	5.4774	LFF	4.8	PN24	7.9773	LFF	52.6
PN11	7.4542	LFF	42.6	PN25	6.1654	LFF	17.9
PN12	8.6522	LFF	65.5	PN26	5.2263	LFF	-0.015
PN13	4.3056	LFF	-17.6	PN27	5.2259	LFF	-0.023
PN14	9.4072	LFF	80	PN28	5.2486	LFF	0.41

The results show that changes in dimensions of the system, its boundary conditions, the rigidity of the main beam, and also adding tie beam, significant changes the FNF of the system up to 133.2%, 52.9%, -52.2%, %52.6%, respectively. In addition, increasing thickness of concrete slab and distance between composite joists increases the FNF of the system up to 6.9% and 4.8%, respectively. Furthermore, the results demonstrate that variation in the rigidity of secondary beam, the height of composite joist, and thickness of the top and bottom flanges of open web steel joists, insignificant changes the FNF of the studied system up to -0.023%, 2.1%, and -0.95%, respectively. Finally, the results uncover that changing in the grade of concrete changes the FNF of the system only by 0.41%.

3.2. STATIC AND DYNAMIC RESPONSES OF THE STUDIED PANELS

Based on the FNFs of the studied panels, the category of the panels (LFF or HFF) was revealed. Then, regarding the main goal of the study, the dynamic analysis was performed to determine peak acceleration of LFFs, and also static and dynamic analysis were performed to determine static stiffness and peak acceleration of HFFs, respectively. Four dynamic load models applied on the studied panels representing human walking load, which described previously. Three paths were considered, as illustrated in Figure 11. The paths show the direction of people who move on the floor. Three damping ratios (1.1%, 3%, and 4.5%) were considered regarding to affirmation of the SCI-P354 [43]. The results of the analysis of the studied panels are presented in Table 5. The obtained accelerations of LFFs and HFFs were compared with the proposed peak acceleration limit by the ISO 2631-2, affirmed by the AISC [7]. Also obtained static stiffness of the HFFs were compared with the proposed minimum static stiffness limit by the AISC (1 kN/mm under concentrated load at the center of the panel).

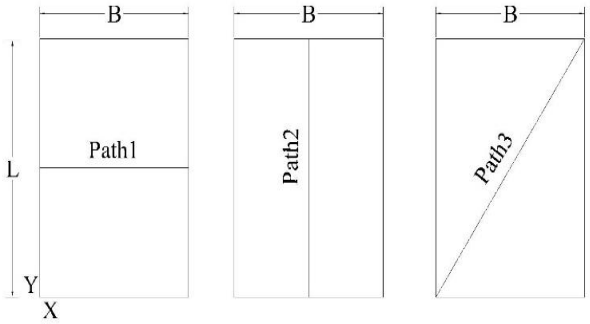

Figure 11. Layout of paths

Table 5. Peak acceleration and static stiffness of studied panels

Panel Number	ξ%	Peak Acceleration									Static Stiffness ($^{kN}/_{mm}$)
		Load I ($^{m}/_{s^2}$)	Load II ($^{m}/_{s^2}$)	Load III ($^{m}/_{s^2}$)			Load IV ($^{m}/_{s^2}$)			ISO 2631-2	
				Path1	Path2	Path3	Path1	Path2	Path3		
PN1	1.1%	0.169	0.362	0.664	1.266	0.919	1.858	1.166	1.99	0.4903	-
	3%	0.101	0.286	0.376	0.233	0.341	0.690	0.823	0.596		
	4.5%	0.073	0.230	0.266	0.579	0.174	0.368	0.690	0.303		
PN2	1.1%	0.104	0.836	0.568	0.39	-	1.145	1.53	-	0.4903	-
	3%	0.087	0.613	0.119	0.182	-	0.155	0.101	-		
	4.5%	0.074	0.488	0.138	0.032	-	0.153	0.064	-		
PN3	1.1%	0.197	0.437	1.24	0.488	-	1.214	0.790	-	0.4903	-
	3%	0.157	0.266	0.386	0.043	-	0.557	0.087	-		
	4.5%	0.127	0.195	0.458	0.012	-	0.296	0.024	-		
PN4	1.1%	0.138	0.363	0.351	0.114	-	0.902	0.803	-	0.4903	-
	3%	0.087	0.218	0.188	0.029	-	0.362	0.144	-		
	4.5%	0.062	0.159	0.106	0.013	-	0.191	0.043	-		
PN5	1.1%	0.450	0.566	0.685	0.248	-	1.926	1.358	-	0.4903	-
	3%	0.251	0.406	0.681	0.292	-	1.117	0.604	-		
	4.5%	0.178	0.311	0.708	0.144	-	1.092	0.260	-		
PN6	1.1%	0.163	0.340	1.066	0.977	-	1.993	1.36	-	0.4903	-
	3%	0.096	0.340	0.404	0.191	-	0.722	0.265	-		
	4.5%	0.069	0.340	0.219	0.057	-	0.386	0.077	-		
PN7	1.1%	0.449	0.567	0.752	0.253	-	1.915	1.365	-	0.4903	-
	3%	0.251	0.406	0.563	0.292	-	1.077	0.604	-		
	4.5%	0.178	0.311	0.496	0.144	-	0.758	0.260	-		
	1.1%	0.402	0.456	0.170	0.173	-	0.458	0.523	-	0.4903	-
PN8	3%	0.065	0.211	0.017	0.020	-	0.091	0.030	-		
	4.5%	0.065	0.146	0.026	0.002	-	0.056	0.007	-		
PN9	1.1%	0.035	0.271	2.079	0.202	-	2.223	0.486	-	0.4903	-
	3%	0.016	0.203	1.169	0.020	-	1.245	0.040	-		
	4.5%	0.011	0.157	0.915	0.004	-	0.987	0.009	-		
PN10	1.1%	0.1886	0.355	1.516	2.461	-	1.934	1.724	-	0.4903	-
	3%	0.109	0.263	0.403	1.577	-	0.614	1.724	-		
	4.5%	0.078	0.197	0.278	1.345	-	0.354	1.724	-		
PN11	1.1%	0.153	0.4	0.641	0.152	-	0.890	0.449	-	0.4903	-
	3%	0.072	0.076	0.547	0.012	-	0.808	0.040	-		
	4.5%	0.053	0.074	0.689	0.021	-	0.756	0.003	-		
PN12	1.1%	0.241	0.291	0.423	0.467	-	0.726	0.564	-	0.4903	-
	3%	0.146	0.154	0.292	0.034	-	0.292	0.058	-		
	4.5%	0.101	0.114	0.422	0.010	-	0.451	0.025	-		
PN13	1.1%	0.396	0.523	2.664	3.813	-	2.251	4.348	-	0.4903	-

	3%	0.266	0.447	2.057	3.525	-	2.513	3.810	-		
	4.5%	0.204	0.438	2.024	3.534	-	2.478	3.800	-		
PN14	1.1%	0.056	0.330	0.600	0.275	-	0.630	0.367	-	0.4903	-
	3%	0.035	0.161	0.599	0.023	-	0.753	0.042	-		
	4.5%	0.019	0.110	0.725	0.004	-	0.901	0.010	-		
PN15	1.1%	0.018	0.253	0.311	0.264	-	0.565	0.552	-	0.4903	15.768
	3%	0.010	0.157	0.454	0.060	-	0.732	0.107	-		
	4.5%	0.007	0.118	0.598	0.033	-	0.883	0.022	-		
PN16	1.1%	0.032	0.259	0.608	0.362	-	0.444	1.242	-	0.4903	20.938
	3%	0.020	0.119	0.078	0.448	-	0.131	1.132	-		
	4.5%	0.013	0.080	0.025	0.606	-	0.035	1.114	-		
PN17	1.1%	0.256	0.528	0.553	0.162	-	1.318	0.617	-	0.4903	-
	3%	0.192	0.324	0.190	0.009	-	0.454	0.072	-		
	4.5%	0.156	0.237	0.164	0.002	-	0.284	0.026	-		
PN18	1.1%	4.3e-4	4.3e-4	1.940	1.386	-	2.239	1.562	-	0.4903	-
	3%	4e-4	4e-4	1.686	0.510	-	1.960	0.771	-		
	4.5%	3.9e-4	3.9e-4	1.750	0.410	-	1.919	0.833	-		
PN19	1.1%	0.095	0.630	0.825	0.280	-	1.325	0.089	-	0.4903	-
	3%	0.045	0.344	0.393	0.001	-	0.767	0.004	-		
	4.5%	0.032	0.242	0.388	3.2e-4	-	0.718	6.5e-4	-		
PN20	1.1%	6.8e-4	6.8e-4	1.061	0.505	-	1.593	0.505	-	0.4903	8960.5
	3%	6.5e-4	6.5e-4	0.849	0.406	-	1.512	0.410	-		
	4.5%	6.5e-4	6.5e-4	0.838	0.389	-	1.515	0.382	-		
PN21	1.1%	0.133	0.216	0.960	0.905	-	1.337	0.985	-	0.4903	-
	3%	0.048	0.145	1.019	0.301	-	1.439	0.357	-		
	4.5%	0.019	0.113	0.966	0.129	-	1.399	0.156	-		
PN22	1.1%	0.018	0.163	0.123	0.068	-	0.164	0.104	-	0.4903	-
	3%	0.045	0.106	0.129	0.012	-	0.149	0.014	-		
	4.5%	0.061	0.079	0.115	0.003	-	0.12	0.047	-		
PN23	1.1%	0.096	0.193	0.070	0.256	-	0.147	0.417	-	0.4903	-
	3%	0.053	0.156	0.016	0.007	-	0.103	0.011	-		
	4.5%	0.037	0.126	0.012	0.001	-	0.057	0.002	-		
PN24	1.1%	0.079	0.201	0.675	0.245	-	0.743	0.414	-	0.4903	-
	3%	0.038	0.136	0.644	0.014	-	0.707	0.016	-		
	4.5%	0.025	0.102	0.601	0.002	-	0.661	0.003	-		
PN25	1.1%	0.399	0.501	0.641	0.326	-	0.759	0.377	-	0.4903	-
	3%	0.250	0.276	0.488	0.074	-	0.515	0.125	-		
	4.5%	0.198	0.198	0.465	0.029	-	0.481	0.048	-		
PN26	1.1%	0.172	0.361	0.665	1.276	-	1.851	1.156	-	0.4903	-
	3%	0.103	0.288	0.420	0.242	-	0.696	0.835	-		
	4.5%	0.073	0.230	0.383	0.069	-	0.515	0.580	-		
PN27	1.1%	0.173	0.361	0.666	1.15	-	1.85	1.284	-	0.4903	-
	3%	0.104	0.287	0.438	0.241	-	0.692	0.836	-		
	4.5%	0.074	0.230	0.337	0.068	-	0.393	0.581	-		
PN28	1.1%	0.107	0.368	0.675	1.081	-	1.853	1.395	-	0.4903	-
	3%	0.069	0.288	0.324	0.267	-	0.694	0.892	-		

Table 5 presents a lot of information about the effect of various parameters on the static and dynamic response of the studied system. Therefore, the PN1 is selected to present the base results of the study. According to Table 5, the peak accelerations of the studied panels were evaluated under the second load model, which uncovered to be greater than those corresponding evaluated peak accelerations under the first load model. This point revealed that considering four harmonics in the dynamic load is a very important issue in the dynamic responses of the floor and showed a significant effect on the increase of the peak acceleration. As it is obvious from Table 5, when the third and fourth load models were applied to the studied panels, the peak accelerations were higher than those of the applied first and second load models. This fact was highlighted when the position of the dynamic load changed across the individual direction, the dynamic response of the panels increased. Gandomkar et al. and Mello et al. also focused on this point and stated that this is a substantial

increase in the structure [39-41]. The peak acceleration of the panels under the fourth load model was assessed higher than those under the third load model. On the other hand, the scheme of loading on the panels in the third and fourth load models was the same as each other. Therefore, this increase should be caused by the heel impact factor ($f_{mi} = 1.12$) used in the fourth load model. In addition, the results demonstrate that increasing of damping ratio has a significant direct effect on decreasing peak acceleration of the system. By comparing the peak acceleration of the PN1 for various considered paths, the results show that the type of path has not distinguished effect on the results. In accordance with the peak accelerations of the studied panels, when the first and second load models apply to them, some panels are comfort for the users, and some of them are not comfortable. This situation is depending on characteristics, boundary conditions, and damping ratio of the panel (Table 5). In addition, by comparing the peak accelerations of the panels under the third and fourth load models with recommendations of the ISO 2631-2, it is uncovered that all panels are not comfortable for the users [6]. The results of the study with focusing on the type of dynamic load model (I, II, III, and IV) demonstrate that changing in the characteristics of the Chromite floor system changes its dynamic response with different phenomena. It means, percent of increase or decrease in peak acceleration of the system under mentioned loads do not have specific rule the same as each other. Therefore, the effect of applying each different dynamic load model (I, II, III, IV) on the results of the study should be investigated independently. For example, by comparing peak acceleration of PN1 (as the base model) with peak acceleration of other panels when the fourth load model (path 2, 3% damping) apply on them, the results show that changing dimension of panel, boundary conditions, rigidity of the main beam, adding tie beam, thickness of concrete slab, rigidity of the secondary beam, height of composite joist, space between the joists, thickness of top and bottom plates of girder, grade of concrete changes peak acceleration of the system up to 6.32%, 26.61%, 98.3%, 98.06%, 82.50%, -1.58%, 91.25%, -109.48%, 89.43%, -8.38%, respectively. Furthermore, by comparing peak acceleration of PN1 with peak accelerations of PN5, PN6, PN7, PN8, and PN9, it is obvious that release sliding in support can decrease the peak acceleration of the system. Also, comparing the peak accelerations of the studied panels in various paths (1, 2, and 3) shows different phenomena. So that, the prediction of peak acceleration under various types of the path is not possible. Moreover, the results show that all high-frequency Chromite panels have enough static stiffness.

4. CONCLUSION

This paper investigates the static and dynamic response of low and high-frequency Chromite floor system under the human walking load to evaluate its comfortableness. Four dynamic load models were used while the third and fourth load models were more pragmatic, having two properties; changing load according to the individual position, and generating time function corresponding to the nature of the human walking load. The effect of the human heel impact was also considered in the fourth load model. Dynamic responses of the low-frequency Chromite panels were obtained in terms of the peak acceleration and compared with the proposed limiting value by the ISO 2631-2 where the panels used as residences and offices. In addition, static and dynamic responses of the high-frequency Chromite panels were determined and compared with the limiting value of the ISO 2631-2 and the AISC [6-7]. Some of the studied panels were shown to be comfortable for users when the first and second dynamic load models applied to them. Also, some of them were not comfortable for users. The position of loads was changed across the individual directions when the third and fourth dynamic load models were applied on the panels. For these two types of load models, three paths were selected to show the effect of moving direction on the dynamic response of the panels. The peak accelerations of the studied panels under the third and fourth dynamic load models were determined higher than those of the first and second loads and also limiting the value of the ISO 2631-2 [6]. Therefore, all panels were not comfortable for users when the third and fourth load models applied to them. These results uncovered this fact that changing the position of the load is an effective item in increasing of the response of the panels. Changing the characteristics of the studied system can change its peak acceleration. In this case, changing the panel's dimension, boundary conditions, the rigidity of the main beam, adding tie beam, the thickness of the concrete slab, the height of composite joist, and space between the joists changes significant peak acceleration of the system. On the other hand, they were changing the secondary beam's rigidity, and the grade of concrete did not change the peak acceleration of the system significantly. Enhancement of the damping ratio of the Chromite system can considerably reduce the peak acceleration of the system. These results can be useful to help designers to reduce the response of the Chromite floor by using suitable furniture and type of partitions [7].

FUNDING/SUPPORT

Not mentioned any Funding/Support by authors.

ACKNOWLEDGMENT

Not mentioned by authors.

AUTHORS CONTRIBUTION

This work was carried out in collaboration among all authors.

CONFLICT OF INTEREST

The author (s) declared no potential conflicts of interests with respect to the authorship and/or publication of this paper.

5. REFRENCES

[1] Ellingwood B, Tallin A. Structural serviceability: floor vibrations. Journal of Structural engineering. 1984 Feb;110(2):401-18. [View at Google Scholar]; [View at Publisher].

[2] Ad Hoc Committee on Serviceability Research, Structural serviceability: A critical appraisal and research needs. Journal of Structural Engineering. 1986;112:2646-2664. [View at Publisher].

[3] Alvis SR. An experimental and analytical investigation of floor vibrations. M.Sc. Thesis, Virginia Polytechnic Institute and State University. 2001. [View at Google Scholar]; [View at Publisher].

[4] Pavic A, Reynolds P. Vibration serviceability of long-span concrete building floors. Part 1: Review of background information. Shock and Vibration Digest. 2002 May;34(3):191-211. [View at Google Scholar]; [View at Publisher].

[5] Gandomkar FA. Determining comfort level of profiled steel sheeting dry board floor system. Ph.D Thesis, Department of Civil Engineering, Universiti Kebangsaan Malaysia. 2012.

[6] ISO 2631-2. Evaluation of human exposure to whole-body vibration Part2: Continuous and shock-induced vibration in buildings (1-80 Hz). International Standards Organization. 1989. [View at Publisher].

[7] American Institute of Steel Construction (AISC). Floor vibration due to human activity: 11th Steel Design Guide Series. 1997. [View at Publisher].

[8] An Q, Ren Q, Liu H, Yan X, Chen Z. Dynamic performance characteristics of an innovative cable supported beam structure–concrete slab composite floor system under human-induced loads. Engineering Structures. 2016 Jun 15;117:40-57. [View at Google Scholar]; [View at Publisher].

[9] Gaspar CM, da Silva JS, Costa-Neves LF. Multimode vibration control of building steel–concrete composite floors submitted to human rhythmic activities. Computers & Structures. 2016 Mar 1;165:107-22. [View at Google Scholar]; [View at Publisher].

[10] Weckendorf J, Toratti T, Smith I, Tannert T. Vibration serviceability performance of timber floors. European Journal of Wood and Wood Products. 2016 May 1;74(3):353-67. [View at Google Scholar]; [View at Publisher].

[11] Zhou X, Cao L, Chen YF, Liu J, Li J. Experimental and analytical studies on the vibration serviceability of pre-stressed cable RC truss floor systems. Journal of Sound and Vibration. 2016 Jan 20;361:130-47. [View at Google Scholar]; [View at Publisher].

[12] Carmona JE, Avila SM, Doz G. Proposal of a tuned mass damper with friction damping to control excessive floor vibrations. Engineering Structures. 2017 Oct 1;148:81-100. [View at Google Scholar]; [View at Publisher].

[13] Friehe M, Heinemeyer C, Feldmann M. Design of highly sensitive floors for human induced vibrations. Procedia engineering. 2017 Jan 1;199:2796-801. [View at Google Scholar]; [View at Publisher].

[14] Shahabpoor E, Pavic A, Racic V. Structural vibration serviceability: New design framework featuring human-structure interaction. Engineering Structures. 2017 Apr 1;136:295-311. [View at Google Scholar]; [View at Publisher].

[15] Andrade P, Santos J, Maia L. Reinforcement Measures to Reduce the Human Induced Vibrations on Stair Steps–A Case Study. Procedia Structural Integrity. 2017 Jan 1;5:1310-7. [View at Google Scholar]; [View at Publisher].

[16] Zhang S. Vibration serviceability of cold-formed steel floor systems. Ph.D Thesis, University of Waterloo. 2017. [View at Google Scholar]; [View at Publisher].

[17] Zhang S, Xu L, Qin J. Vibration of lightweight steel floor systems with occupants: modelling, formulation and dynamic properties. Engineering Structures. 2017 Sep 15;147:652-65. [View at Google Scholar]; [View at Publisher].

[18] Mohammed AS, Pavic A, Racic V. Improved model for human induced vibrations of high-frequency floors. Engineering Structures. 2018 Aug 1;168:950-66. [View at Google Scholar]; [View at Publisher].

[19] Casagrande D, Giongo I, Pederzolli F, Franciosi A, Piazza M. Analytical, numerical and experimental assessment of vibration performance in timber floors. Engineering Structures. 2018 Aug 1;168:748-58. [View at Google Scholar]; [View at Publisher].

[20] Do NT, Gül M, Abdeljaber O, Avci O. Novel framework for vibration serviceability assessment of stadium grandstands considering durations of vibrations. Journal of Structural Engineering. 2018 Feb 1;144(2):04017214. [View at Google Scholar]; [View at Publisher].

[21] Campista FF, da Silva JG. Vibration analysis of steel–concrete composite floors when subjected to rhythmic human activities. Journal of Civil Structural Health Monitoring. 2018 Nov 1;8(5):737-54. [View at Google Scholar]; [View at Publisher].

[22] Cao LL, Qian C, Chu LZ, Yu GJ. A Review of Research on Human-induced Vibration Serviceability and Dynamic Properties of Long-span Floor. InE3S Web of Conferences 2018 (Vol. 38, p. 03012). EDP Sciences. [View at Google Scholar]; [View at Publisher].

[23] Zhou X, Yang Q, Li J, Ma X. Human-induced vibration serviceability of arch pre-stressed concrete truss system. Journal of Measurements in Engineering. 2018 Dec 31;6(4):263-70. [View at Google Scholar]; [View at Publisher].

[24] Chen S, Zhang R, Zhang J. Human-induced vibration of steel–concrete composite floors. Proceedings of the Institution of Civil Engineers-Structures and Buildings. 2018 Jan;171(1):50-63. [View at Google Scholar]; [View at Publisher].

[25] Wang X. Vibration control strategies for cancelling floor vibration via inertial mass dampers. Ph.D Thesis, Departamento de Mecanica de Medios Continuos y Teoria de Estructuras, Universidad Politecnica de Madrid. 2018. [View at Google Scholar]; [View at Publisher].

[26] Hassanieh A, Chiniforush AA, Valipour HR, Bradford MA. Vibration behaviour of steel-timber composite floors, part (2): evaluation of

human-induced vibrations. Journal of Constructional Steel Research. 2019 Jul 1;158:156-70. [View at Google Scholar]; [View at Publisher].

[27] Chiniforush AA, Alamdari MM, Dackermann U, Valipour HR, Akbarnezhad A. Vibration behaviour of steel-timber composite floors, part (1): Experimental & numerical investigation. Journal of Constructional Steel Research. 2019 Oct 1;161:244-57. [View at Google Scholar]; [View at Publisher].

[28] Ebadi MM, Doudak G, Smith I. Evaluation of floor vibration caused by human walking in a large glulam beam and deck floor. Engineering Structures. 2019 Oct 1;196:109349. [View at Google Scholar]; [View at Publisher].

[29] Abdeljaber O, Hussein M, Avci O, Davis B, Reynolds P. A novel video-vibration monitoring system for walking pattern identification on floors. Advances in Engineering Software. 2020 Jan 1;139:102710. [View at Google Scholar]; [View at Publisher].

[30] Gonçalves MS, Pavic A, Pimentel RL. Vibration serviceability assessment of office floors for realistic walking and floor layout scenarios: Literature review. Advances in Structural Engineering. 2020 Apr;23(6):1238-55. [View at Google Scholar]; [View at Publisher].

[31] Royvaran M, Avci O, Davis B. Analysis of floor vibration evaluation methods using a large database of floors framed with W-Shaped members subjected to walking excitation. Journal of Constructional Steel Research. 2020 Jan 1;164:105764. [View at Google Scholar]; [View at Publisher].

[32] Huang H, Gao Y, Chang WS. Human-induced vibration of cross-laminated timber (CLT) floor under different boundary conditions. Engineering Structures. 2020 Feb 1;204:110016. [View at Google Scholar]; [View at Publisher].

[33] Li Z, Zhang Q, Fan F, Shen S. A method for calculating uncomfortable rates of people due to vertical floor vibrations using corresponding assessment values based on fuzzy reliability theory. Journal of Building Engineering. 2020 Mar 1;28:101061. [View at Google Scholar]; [View at Publisher].

[34] Zhang X, Wang Q, Wang Y, Li Q. Experimental and Analytical Study on the Vibration Performance of U-Shaped Steel-Concrete Composite Hollow Waffle Slab. Shock and Vibration. 2020 Feb 27;2020. [View at Google Scholar]; [View at Publisher].

[35] Middleton CJ, Brownjohn JM. Response of high frequency floors: A literature review. Engineering Structures. 2010 Feb 1;32(2):337-52. [View at Google Scholar]; [View at Publisher].

[36] Ljunggren F, Wang J, Ågren A. Human vibration perception from single-and dual-frequency components. Journal of Sound and Vibration. 2007 Feb 20;300(1-2):13-24. [View at Google Scholar]; [View at Publisher].

[37] BS 8110. Part1: Code for practice for design and construction. Structural use of concrete. British Standards Institution. 1997. [View at Google Scholar]; [View at Publisher].

[38] da Silva JS, da S Vellasco PC, De Andrade SA, da CP Soeiro FJ, Werneck RN. An evaluation of the dynamical performance of composite slabs. Computers & Structures. 2003 Aug 1;81(18-19):1905-13. [View at Google Scholar]; [View at Publisher].

[39] Gandomkar FA, Badaruzzaman WH, Osman SA. Dynamic response of low frequency Profiled Steel Sheet Dry Board with Concrete infill (PSSDBC) floor system under human walking load. Latin American Journal of Solids and Structures. 2012;9(1):21-41. [View at Google Scholar]; [View at Publisher].

[40] Gandomkar FA, Badruzzaman WH, Osman SA, Ismail I. Dynamic response of low frequency Profiled Steel Sheet Dry Board (PSSDB) floor system. Latin American Journal of Solids and Structures. 2013 Nov;10(6):1135-54. [View at Google Scholar]; [View at Publisher].

[41] Mello AD, Da Silva JG, Vellasco PD, De Andrade SA, De Lima LR. Dynamic analysis of composite systems made of concrete slabs and steel beams. Journal of Constructional Steel Research. 2008 Oct 1;64(10):1142-51. [View at Google Scholar]; [View at Publisher].

[42] Abaqus Analysis User's Manual Version 6.12. [View at Publisher].

[43] Smith AL, Hicks SJ, Devine PJ. Design of floors for vibration: A new approach. Ascot, Berkshire, UK: Steel Construction Institute; 2007. [View at Google Scholar]; [View at Publisher].